

## ARTICLE / INVESTIGACIÓN

# Synthesis and characterization of seed-based Carbon Black Agglomerates: Application as sorbent material using a novel microextraction technique for dexamethasone in urine sample determination

E.M. Ordoñez López<sup>1</sup>, Y.N. Baca García<sup>2</sup>, F.A. Ordoñez Trochez<sup>2</sup>, K.A. Barahona Montes<sup>2</sup>, F.A. Rodríguez Rivas<sup>1</sup>, H.D. Ponce-Rodríguez<sup>2\*</sup>

DOI. 10.21931/RB/2023.08.03.39

<sup>1</sup> Departamento de Química, Facultad de Ciencias Químicas y Farmacia, Universidad Nacional Autónoma de Honduras, Tegucigalpa, Honduras.<sup>2</sup> Departamento de Control Químico, Facultad de Ciencias Químicas y Farmacia, Universidad Nacional Autónoma de Honduras, Tegucigalpa, Honduras.Corresponding author: [henry.ponce@unah.edu.hn](mailto:henry.ponce@unah.edu.hn)

**Abstract:** The growing development of Nanotechnology has allowed the synthesis and characterization of nanomaterials with peculiar physicochemical properties. These nanomaterials have been applied in various scientific and industrial sectors. The present study established the synthesis of carbon black agglomerates (CBA) from waste vegetal materials as a source of renewable raw materials using a simple, fast, and effective procedure. Once this nanostructured material was obtained, several analytical techniques were applied to establish its main characteristics, including X-ray diffraction, Fourier transform infrared spectroscopy, Brunauer–Emmett–Teller (BET) theory analysis, and SEM imaging. The results of this characterization have made it possible to establish that these materials have properties that make them suitable for application as extracting sorbents in microextraction sample treatment techniques under the green analytical chemistry approach. In this study, we applied Pipette-tip SPE microextraction for pharmaceutical compound extraction studies, preparing extraction devices with less than five milligrams of the sorbent. The results showed high extraction percentages for compounds such as paracetamol, caffeine, diazepam, and dexamethasone. Finally, an application example of the last compound is presented, developing a procedure for its determination in urine samples by high-performance liquid chromatography with diode array detection (HPLC-DAD) chromatographic analysis with high merit figures in terms of simplicity, high extraction efficiency, and environmental friendliness.

**Key words:** Carbon black, nanostructured material, olive seed, microextraction, biological samples.

## Introduction

In recent years, the application of nanotechnology in various fields of science has increased exponentially, with the study of the structures of matter on a scale of a billionth of a meter. According to the European Commission Recommendation 2022/C229/01, a 'nanomaterial' is a natural, incidental, or manufactured material consisting of solid particles that are present, either on their own or as identifiable constituent particles in aggregates or agglomerates, and where 50% or more of these particles in the number-based size distribution fulfill at least one of the following conditions: (a) the external dimensions of the particle are in the size range 1 nm to 100 nm; (b) the particle has an elongated shape, such as a rod, fiber, or tube, where two external dimensions are smaller than 1 nm and the other dimension is more significant than 100 nm; and (c) the particle has a plate-like shape, where one external dimension is smaller than 1 nm and the other dimensions are more significant than 100 nm<sup>1</sup>. Nanoparticles (NPs) are small molecular aggregates with an interfacial layer surrounding a diameter of one to 100 nanometers<sup>2</sup>. The small size of NPs makes them possess unusual properties compared with bulk materials, which is why they have been used in many applications such as disease treatment, biomedical instrumentation, drug and gene delivery, nanosensors, and biomarkers.

Among the many NPs, the most used are Metallic NPs<sup>3</sup>, Quantum Dots(QDs)<sup>4</sup>, Carbon-based NMs (C-NMs)<sup>5</sup>, and Silica-based NMs<sup>6</sup>.

Carbon black nanoparticles (CBN) are a fine powder of manufactured amorphous material, almost elemental Carbon, in spherical particles and their agglomerates and agglomerations. The incomplete and oxygen-reduced combustion of biomass residues<sup>7</sup> obtains these nanoparticles. Certain fundamental properties of Carbon black include particle size, structure, porosity, surface activity, and physical form. Thus, CB's molecular adsorption largely depends on its surface area, high microporosity, and material source. In addition, CBN is cheaper than other carbon materials such as carbon nanotubes and graphene, which has allowed it to be widely applied as sorbent material<sup>8,9</sup> and for the development of low-cost electrochemical sensors<sup>10,11</sup>. The main difference between CB and black Carbon (elemental Carbon) is the lower content of extractable organic and inorganic compounds (less than 1%)<sup>12</sup>.

Moreover, both have physical-chemical differences because the latter is generated as an incomplete combustion by-product, with carbon content in its structure lower than 50%<sup>13</sup>. Since the production process for the synthesis of CBNs directly affects their properties and performance, it

**Citation:** Ordoñez López E M; Baca García Y N; Ordoñez Trochez F A; Barahona Montes K A; Rodríguez Rivas F A; Ponce-Rodríguez H D. Synthesis and characterization of seed-based Carbon Black Agglomerates: Application as sorbent material using a novel microextraction technique for dexamethasone in urine sample determination, *Revis Bionatura* 2023;8 (3) 39. <http://dx.doi.org/10.21931/RB/2023.08.03.39>

**Received:** 20 June 2023 / **Accepted:** 25 August 2023 / **Published:** 15 September 2023

**Publisher's Note:** Bionatura stays neutral with regard to jurisdictional claims in published maps and institutional affiliations.

**Copyright:** © 2022 by the authors. Submitted for possible open access publication under the terms and conditions of the Creative Commons Attribution (CC BY) license (<https://creativecommons.org/licenses/by/4.0/>).



should be noted that there are three main processes, from those of incomplete combustion, such as thermal oxidative decomposition that includes furnace black, lampblack, and channel black<sup>14</sup>. On the other hand, the thermal decomposition process in the absence of oxygen, including thermal black and acetylene black, and finally, the plasma process, represents the most environmentally friendly method<sup>15</sup>. The average size of the CB particles ranges from 3.0 to 100 nm. The formation of aggregate nanostructures, which are semispherical groups, is one of the characteristics of CB. Moreover, these large aggregate groups can form agglomerates<sup>16</sup>.

In recent years, essential issues within green chemistry have involved reducing waste generation and its treatment and the recovery of waste that promotes the use of renewable raw materials. Plaza et al. mentioned that biomass residues, mostly from agricultural activities, have been widely used as feedstock to produce activated carbon<sup>17</sup>. A study has shown that the residual biomass of olive groves and the olive oil industry is an accessible feedstock for obtaining activated carbon<sup>18</sup>. Likewise, a successful strategy to prepare added-value porous carbons from banana peel waste (BPW) as a biomass precursor was reported by Luna-Lama et al.<sup>19</sup>. More recently, Lian et al. reported using rice straw to prepare CB nanoparticles for phenanthrene sorption studies<sup>20</sup>. The physical-chemical characterization of carbon black nanoparticles obtained from biomass uses different approaches, including structural, chemical, and textural characterization. Determining morphology allows the characterization of particle core sizes and shapes; therefore, image techniques such as transmission electron microscopy (TEM) and scanning electron microscopy (SEM) have been applied. Other key parameters for assessing the structural modification, functionalization, and applicability of CBA are structural information, crystallinity, and graphite content. Several analytical techniques have been documented in the literature, including Fourier transform infrared spectroscopy (FTIR), thermogravimetric analysis (TGA), Raman spectroscopy, X-ray diffraction (XRD), and photoelectronic X-ray Spectroscopy (XPS) for this purpose<sup>21-23</sup>. Despite the benefits of the abovementioned techniques, none simultaneously provide particle size characterization with size-dependent separation and quantification. In that line, asymmetrical flow field-flow fractionation (AF4) provides information to evaluate the presence or absence of several NP distributions according to particle properties such as size, composition, or electrophoretic mobility<sup>24,25</sup>.

Developing new microextracción techniques has involved an essential topic in green analytical chemistry, many of which have been developed on a miniaturized scale. In this sense, applying new and better sorbent materials represents an important research topic for improving the efficiency and tuning extraction selectivity<sup>26,27</sup>. A new variant of the traditional solid-phase extraction (SPE) technique is called "Pipettips SPE (PT-SPE)," which is a miniaturized format of SPE that facilitates automated systems using available tools in many laboratories<sup>28</sup>. In this technique, the pipette tip carries the sorbent material and has a fine slit at its bottom, allowing the liquid phase to pass. In contrast, the chromatographic material remains in the tip. The main green characteristics of PT-SPE involve reducing the sorbent amount, which contributes to reducing the amount of organic solvents used, lowering costs, and performing Eco-Friendly extraction<sup>29</sup>. Dexamethasone sodium phosphate, a glucocorticoid derivative of hydrocortisone, is a synthetic version

of a natural hormone produced in the adrenal glands<sup>30</sup>. This molecule has potent anti-inflammatory activity and is widely used to treat inflammatory conditions, allergic reactions, shock, lymphoma, and diseases associated with adrenal cortex insufficiency. Once administered, dexamethasone is rapidly absorbed, and up to 65% of the dose is excreted in the urine within 24h<sup>31</sup>. The analytical methodologies used for dexamethasone determination in biological samples include GC-MS, although a derivatization step is required<sup>32</sup>. Therefore, liquid chromatography with UV or MS detection is most commonly applied<sup>33,34</sup>. Regarding sample treatment techniques, the literature reports the application of solid-phase extraction<sup>35</sup>, pressurized liquid extraction (PLE)<sup>36</sup>, and dispersive liquid-liquid microextraction based on solidifying floating organic drop (DLLME-SFO)<sup>37</sup>.

In this context, our study presents the synthesis of CB agglomerates of vegetal origin using olive stone by-products from the olive oil industry as a raw material. Characterization studies involve various analytical techniques, such as X-ray diffraction, IR spectroscopy, BET, and SEM. For the second stage, CBA is applied as a sorbent material to develop a new variation of the PT-SPE microextraction technique, with figures of merit in terms of the amount of sorbent used, reduced use of solvents, easy automation, high reproducibility, and adequate precision, in line with the principles of green analytical chemistry. Finally, the proposed methodology is applied to adsorption studies of several pharmaceutical compounds with diverse physicochemical properties, including paracetamol, caffeine, lidocaine, diazepam, losartan, valsartan, irbesartan, atorvastatin, and dexamethasone. Concerning the latter compound, its determination in human urine samples is presented as a practical application.

## Materials and methods

### Chemicals and solutions

All reagents used were of analytical grade. Formic acid, sulfuric acid, MnAc<sub>2</sub>·4H<sub>2</sub>O, LiAc·1/3H<sub>2</sub>O, zinc chloride, polyethylene glycol, and potassium bromide (FTIR grade) were purchased from Merck (Darmstadt, HE, Germany). JT Baker (Radnor, PA, USA) supplied HPLC-grade methanol and acetonitrile. Type I ultrapure water obtained with purifying equipment from Thermo Scientific model Barnstead MicroPure ST (Waltham, MA, USA) was used in the experiments. Paracetamol, caffeine, lidocaine, diazepam, dexamethasone, losartan, valsartan, irbesartan, and atorvastatin standards were purchased from Sigma-Aldrich (St. Louis, MO, USA). Individual stock solutions of each compound were prepared at a concentration of one mg/mL by dissolving the exact mass of each compound in methanol. Working solutions of the analyses and their mixtures were prepared by diluting the stock solutions with the appropriate solvent. All solutions were stored at 4°C until use.

### Instruments and analytical conditions

The XRD patterns of the synthesized agglomerates were recorded in a Siemens D5000 diffractometer controlled by a DifraccPlus Basic 4.0 computer system equipped with a graphite monochromator for the diffracted beam and a proportional-type detector. The type of radiation used was CuK $\alpha$  ( $\lambda_1=1.5418 \text{ \AA}$  and  $\lambda_2=1.54439 \text{ \AA}$ ), and the recording conditions were 40 kV and 30 mA in the modality by step

of 3° and 80° (2 $\theta$ ). The step width was 0.02° (2 $\theta$ ), and the recording time was 0.6 s per step.

The IR spectra were obtained using a Perkin-Elmer Spectrum One Fourier transform infrared spectrophotometer connected to a computer with suitable software for data processing. The scan was performed at intervals between 4500 and 400 cm<sup>-1</sup>. The spectrum obtained is the average of forty records that allow improvement of the signal/noise ratio, with a nominal resolution of four cm<sup>-1</sup>. To analyze the agglomerates, tablets with an approximate thickness of 13 mm were prepared and pressed at adequate pressure from a homogeneous mixture formed by 1% of the sample in KBr of analytical quality for FTIR. In the recording of the sample, the background produced by the KBr was subtracted, subtracting from the spectrum of the sample the spectrum produced by a pure tablet of said salt.

The SEM images were obtained using a JEOL JSM 6300 scanning electron microscope, consisting of a secondary electron detector that provides topographic images of the sample's surface previously dehydrated and covered by a thin metal layer. The Autosorb-iQ-MP/MP-XR device obtained surface area data, automatically providing isotherms. Using ASiQwin software, the BET method was applied to the isotherms to obtain the specific surface values of the samples. Likewise, the program calculates the pore distribution from the adsorption and desorption branches. Previously, the samples were subjected to degassing to eliminate all adsorbed water. This treatment was performed at 110 °C, and its duration depended on the sample's surface.

For the development of the adsorption studies and analysis of the urine samples, the following equipment was used: a centrifuge for 50 mL capacity tubes (LW Scientific brand, model C5; Lawrenceville, GA, USA), an ultrasonic bath (Branson<sup>TM</sup> brand, model C5, CPX2800; Ferguson, MO, USA). A mechanical stirrer from KoolLab, model KSV-VM-1000 (Miami, FL, USA), and a vacuum pump from Millipore, model WP6111560 (Burlington, MA, USA). Standards, reagents, and CBA were weighed on an OHAUS Explorer Pro model analytical balance (Parsippany, NJ, USA). The extraction procedure was performed in an Agilent Technologies (Santa Clara, CA, USA) solid-phase extraction chamber. For the spectroscopic studies, a double-beam spectrophotometer, Shimadzu model UV-1800 (Nakagyo-ku, Kyoto, Japan), was equipped with a deuterium lamp and a tungsten filament lamp. Quartz cells with an optical path length of 10 mm were used for the measurements. Acquisition and data treatment were performed using UVprobe software version 2.7 (Shimadzu).

The chromatographic studies were performed in a Shimadzu liquid chromatograph Prominence model (Nakagyo-ku, Kyoto, Japan) equipped with a DGU-20A5 degasser, SIL-20A automatic injector, CTO-A20 column oven, and LC20-model pump. AT, CMB-20Alite control system, and SPD-M20A diode array detector. EZstart software version 7.4 (Shimadzu) was used for the acquisition and data system. A 15-cm C18 XDB column with an internal diameter of 4.6 mm and a particle size of 5  $\mu$ m from Agilent (Santa Clara, CA, USA) was used for the chromatographic separation. The mobile phase consists of a mixture of water (A) and acetonitrile (B) (85:15, v/v) in gradient elution mode: 15% B at 0 min, held for 4 min, and 70% at 5 min. Subsequently, this percentage was maintained for 3 min and decreased to 15% after 3 min. Finally, the initial conditions were obtained in 2 min with a stabilization stage of 2 min. The total analysis time was 19 min, and the dexamethasone signal appeared

at 12 min. The flow rate of the mobile phase was 1 mL/min, with an injection volume of 25  $\mu$ L for the standard and sample solutions. The analyses were performed at room temperature. The maximum absorption of the dexamethasone signal was recorded at 240 nm.

### Carbon Black Agglomerate Synthesis

The synthesis of carbon black agglomerates was performed according to a procedure previously reported by Caballero *et al.*<sup>38</sup> with some modifications related to the time of the final stage of heating at 800 °C for three and a half hours. After the isolation of the solid residues, the olive pits were cleaned and dried in a rotary oven at 200 °C, followed by carbonization at 700 °C and activation under steam. The material was then ground to a fine black powder and dried at 120 °C. After treatment with dilute H<sub>2</sub>SO<sub>4</sub> and washing with abundant distilled water, the material was impregnated with an activating agent solution consisting of an aqueous solution of ZnCl<sub>2</sub> for 7 h. The impregnation ratio was 1 g ZnCl<sub>2</sub> / 4 g initial material. Subsequently, the product was filtered, washed, dried, and heated to 500 °C at 10 °C / min in a dynamic N<sub>2</sub> atmosphere at a 100 mL/min flow rate. The final temperature was maintained for 2 h. Finally, the solid was allowed to cool to room temperature in the oven under a nitrogen atmosphere. Spinel was obtained by mechanical activation of Mn(CH<sub>3</sub>COO)<sub>2</sub>·4H<sub>2</sub>O and Li(CH<sub>3</sub>COO)<sub>3</sub>·3H<sub>2</sub>O in the presence of polyethylene glycol polymer (PEG-400) for 1 h to adapt the size and shape of the particles. Further heating at 800 °C for three and a half hours produced a pure spinel with amorphous agglomerates with a pore size of 2 nm.

### Carbon Black Agglomerates Characterization

The characterization of CBA was performed using X-ray diffraction (XRD), Fourier transform infrared spectroscopy (FTIR), Brunauer, Emmett, and Teller (BET) theory, and scanning electron microscopy (SEM). The instrumental conditions are detailed in the section Instruments and Analytical Conditions. The obtained results are displayed in the Results section.

### PT-SPE device preparation and microextraction procedure

Before optimizing the microextraction procedure, pipette-tip SPE devices were prepared. For this purpose, a small piece of 20  $\mu$ m porosity polyethylene (PE) frit (Merck, Darmstadt, HE, Germany) was placed at the bottom of a 1 mL capacity pipette tip. This type of fruit is usually used to prepare homemade SPE cartridges and allows the solvent to pass through while the sorbent material remains in the tip. Subsequently, the amount of CBA was weighed on an analytical balance and placed inside the pipette tip to close the upper part of the tip with paraffin paper. Table S1 of the Supplementary Material shows the weights obtained in preparing PT-SPE. In Figure 1.A, the preparation of the pipette tips is schematized, while in Figure 1.B, a photograph of the CBA is shown. The typical steps involved in the SPE process include activation, conditioning, loading, cleaning, and elution. In the first, 200  $\mu$ L of methanol is added to activate the surface of the agglomerates. At the same time, in the conditioning, it is sought to pass a solvent with characteristics similar to that of the sample, which is why 200  $\mu$ L of water is added. At the loading stage, 4 mL of blank solutions, standard solutions, and urine samples were passed through the pipette tip. The urine sample was obtained from a heal-

thy volunteer. Then, a cleaning step is required to eliminate the impurities and interferences without eluting the analyte; 100  $\mu\text{L}$  of methanol is added. Finally, 500  $\mu\text{L}$  of acetonitrile was added and collected in an HPLC vial for chromatographic separation to achieve the analyte's elution. All these operations were performed under a vacuum.

## Results

### Characterization of Carbon Black Agglomerates

X-ray diffraction: In this stage, the diffractogram of the carbon black agglomerates is observed to determine the structure of the sample. The gap in Figure 2A shows the very amorphous structure characteristic of this type of compound because it does not have a marked crystalline structure. It is possible to appreciate two broad peaks of low intensity at twenty-five and 43 degrees ( $2\theta$ ) corresponding to the planes (002) and (100) of the Carbon in its graphite phase.

Fourier transform infrared spectroscopy (FTIR): The ac-

tivity of Carbon generally depends on the functional groups in the graphemic sheets. The infrared spectrum (Figure 2.B) is characteristic of this type of compound, with a band observed at  $2929\text{ cm}^{-1}$  corresponding to some vibrations C-H  $1651\text{ cm}^{-1}$  corresponding to vibrations C=C oleophilic, while the skeletal ones in aromatic rings cause the appearance of bands around  $1510$  and  $1425\text{ cm}^{-1}$ . In addition, some small vibrations around  $100$  and  $500\text{ cm}^{-1}$  attributable to Zn vibrations are observed.

BET: According to the BET analysis, a high surface area of the activated Carbon of  $587\text{ M}^2/\text{g}$  is presented due to the microporous nature of the material, confirmed by the small pore size of  $2.27\text{ nm}$ , which confirms the presence of micro/mesoporous structure. The nitrogen adsorption-desorption isotherm in Figure 3 shows, according to the BDDT classification, that the form of adsorption is mixed, type I (typical of microporous system) and type IV at relative pressures higher than  $0.6$  in the desorption branch, which is also indicative of mesoporous systems. The data are summarized in Figure 2.C.

SEM: The SEM images of the carbon black agglomer-

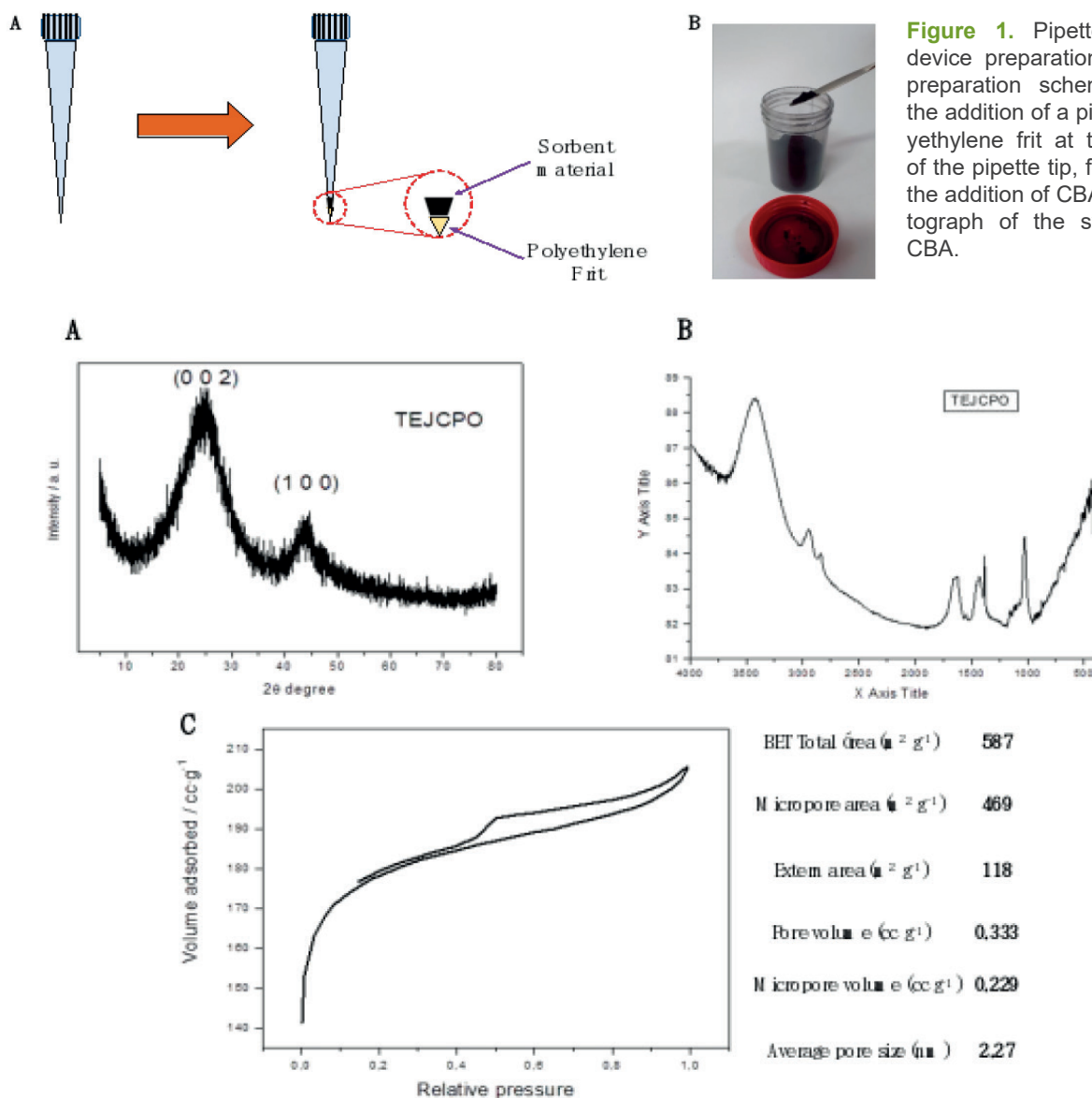


**Figure 2.** Characterization data of carbon black agglomerates (A) X-ray diffractogram (B) IR spectrum (C) N<sub>2</sub> adsorption-desorption curve and BET analysis data.

**Figure 1.** Pipette-tip SPE device preparation. (A) The preparation scheme shows the addition of a piece of polyethylene frit at the bottom of the pipette tip, followed by the addition of CBA. (B) Photograph of the synthesized CBA.

rates exhibit a porous structure of a predominantly microporous character, which results in a high surface area and allows it to possess important characteristics when used as a sorbent material. Consequently, the results of characterization tests reinforce that CBA can be applicable as a sorbent material in microextraction techniques. Figure 3 shows the SEM images of the synthesized CBA.

### Extraction studies

Extraction studies were conducted using solutions of all nine compounds at concentrations of 0.01 mg/mL, except lidocaine at 0.17 mg/mL, prepared in ultrapure water. The first test evaluated if the extraction percentage was affected by the amount of agglomerates used, for which PT-SPE devices with one and 5mg of CBA were prepared. For this, two aliquots of 1 mL of the dexamethasone solution were passed through two extraction devices, one containing 1 mg and the other containing 5 mg of sorbent material. Each aliquot was collected and diluted with 2 mL of water to obtain the absorption spectrum and corresponding absorbance values. A third aliquot of equal volume was diluted with 2 mL of water and measured directly into the spectrophotometer. Figure 4. A shows the absorption spectra obtained, observing that the unextracted solution (black) presents a higher absorbance signal, whereas the solution extracted with 5 mg (red) presents the lowest signal. Finally, the dexamethasone dilution extracted with 1 mg of CBA (green) had an intermediate signal. This test was repeated with the lidocaine solution (Figure 4. B), showing the same behavior as that for dexamethasone. From the absorption spectra results, it is possible to establish that extraction with 5 mg of CBA increases the background signal, which may cause a high matrix effect from the carbon black agglomerates when this quantity is used. According to these results, it was possible to verify that the greater the amount of sorbent material, the greater the percentage of extraction of the compounds. The extraction procedure was performed for all the compounds in triplicate using TP-SPE with 5 mg of sorbent material, and the extraction percentages were calculated, which are summarized in the graph of Figure 4. C.

High extraction values were found for acetaminophen, caffeine, diazepam, and dexamethasone (above 70%), whereas the other compounds presented values lower than

41%, with lidocaine having the lowest percentage (less than 24%). Consistent with the Log Kow data shown in Figure S1 of the Supplementary Material, this behavior does not depend on the molecule's polarity because high-polarity compounds such as caffeine and paracetamol are highly retained in the agglomerates. Conversely, low-polarity molecules such as valsartan and atorvastatin are poorly retained in the sorbent material. In any case, it is possible to establish that, as expected, the CBA does not interact through ionic bonds with the molecules. Instead, it achieves retention of the analyses because of their high porosity, as established in characterization studies.

### Optimization of PT-SPE parameters

Before optimizing the different TP-SPE extraction parameters, chromatographic separation was achieved using the procedure reported by Huang *et al.*<sup>37</sup> With some modifications and obtaining the chromatographic signal of dexamethasone before 12 min. The compound was determined by comparing the resulting absorption spectrum with the theoretical absorption spectrum of dexamethasone. The dexamethasone standard was identified using IRTF (Figure S2 of supplementary material). Based on the results of the extraction studies, initial tests were performed using 5 mg of BCNs in the pipette tip. For activation, 200  $\mu$ L of methanol and 200  $\mu$ L of water were added as the conditioning solvent. To reach the detection limits reported in the literature for dexamethasone in urine, we used 4 mL of the solutions in the loading stage.

Four parameters of the extraction process were optimized: the elution solvent, acidification of the solutions, salting-out effect, and cleaning solvent. Table 1 summarizes the optimized parameters and variables. All tests were performed using standard solutions and fortified urine samples at 200 ng/mL concentration. Two elution solvents, acetonitrile and methanol, were tested. Because the former exhibits a higher elution strength, a more significant signal intensity of the analyte was obtained in the extraction of standard solutions prepared in ultrapure water. The volume of acetonitrile necessary to elute the analyst was established at 500  $\mu$ L; however, elution can be performed using 200  $\mu$ L to lower the detection limits. Two extractions were performed to evaluate the effect of acidifying the solutions on the extraction

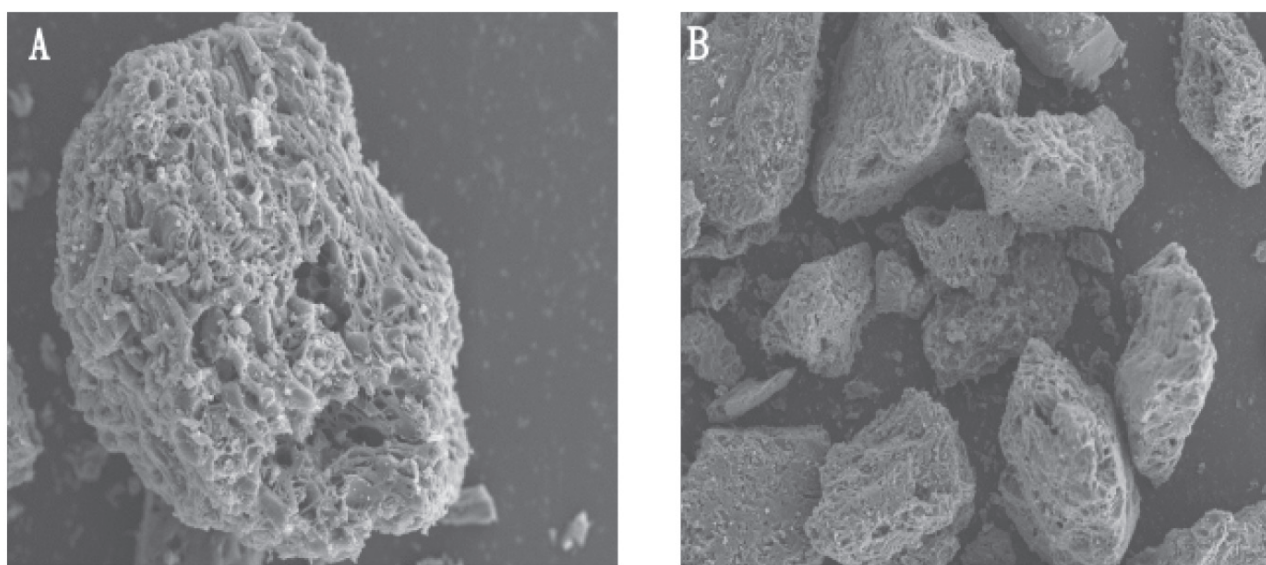
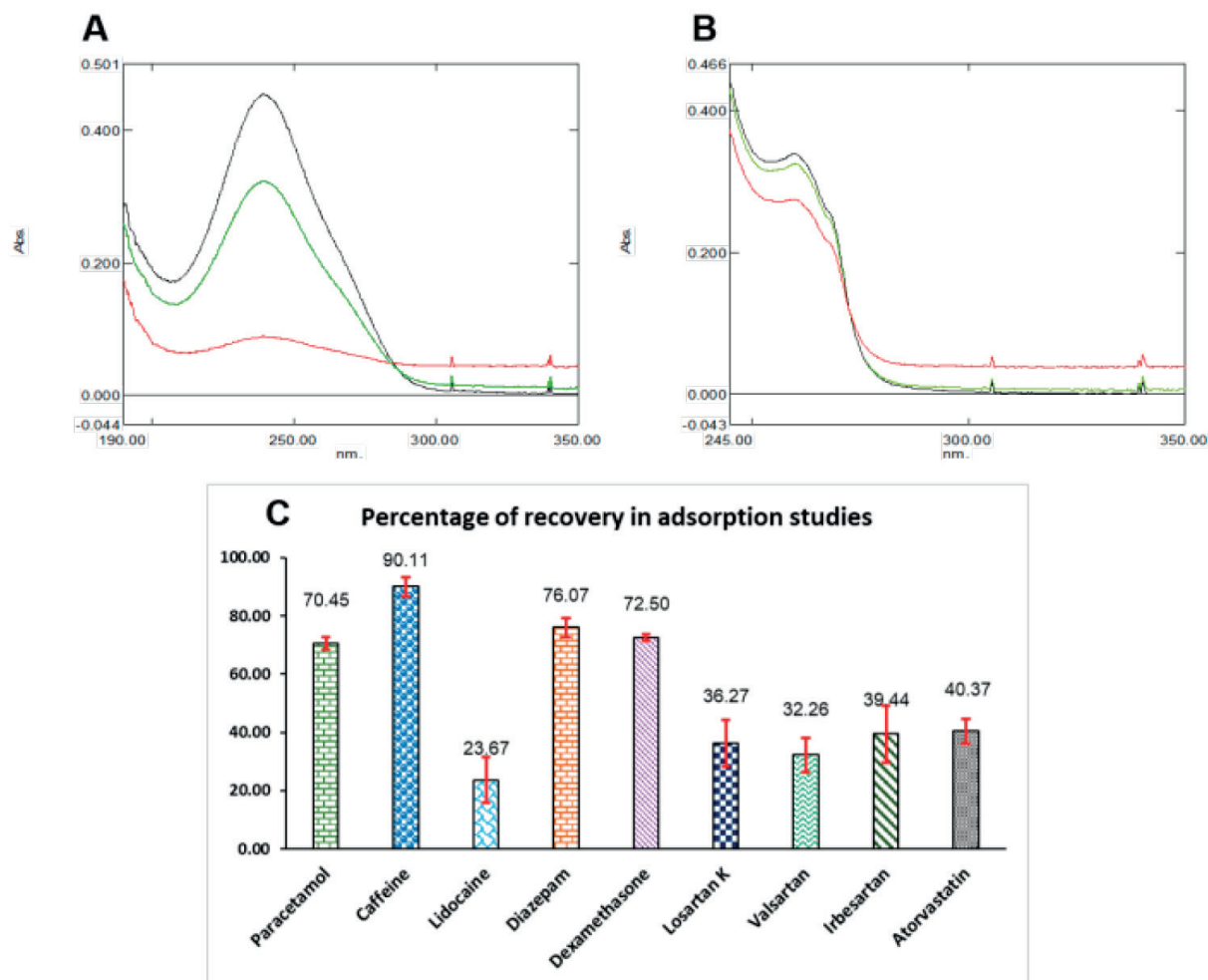


Figure 3. SEM images of carbon black agglomerates. Scale bar A: 200 $\mu$ m; Scale bar B: 600 $\mu$ m.



**Figure 4.** Extraction studies results. (A) Extraction of dexamethasone: unextracted solution (black) extracted with 5mg CBA (red) and extracted with 1mg CBA (green). (B) Extraction of lidocaine: unextracted solution (black), extracted with 5mg CBA (red), and extracted with 1mg CBA (green). (C) Percentage of recovery for all nine compounds, red bars mean SD (n=3). For other experimental details, see the text.

efficiency, one without acidification and the other adding 25  $\mu$ L of formic acid. The signals obtained from both solutions did not show significant differences. This behavior may be because dexamethasone has a pKa value equal to 1.83, with extraction being favored at neutral or slightly acidic pH values. Finally, it was decided to apply the procedure without acidifying the solutions.

The addition of sodium chloride to modify the ionic strength of the sample was evaluated in the same way as acidification, i.e., a solution was prepared without adding the saturated sodium chloride solution (37% w/v). In contrast, 200  $\mu$ L of the saturated solution was added to a second solution. No significant differences were observed in

the signals of both solutions; therefore, we decided not to modify the ionic strength. The last parameter evaluated was the solvent used in the cleaning stage, seeking to use a solvent capable of eliminating most of the interferences retained in the agglomerates without involving the loss of the analyte. Usually, for this purpose, it is adequate to use a solvent with low elution strength, such as methanol or water. These solvents were tested, performing two extractions on a urine sample fortified with dexamethasone, each with 100mL of each solvent. The chromatograms showed lower impurities and interferences when methanol was used without decreasing the analyte signal. Therefore, it was established that the extraction procedure should be performed

Factors	Units	Evaluated values	
		Value 1	Value 2
Elution solvent	Type	Acetonitrile	Methanol
Acidification of the solution	Yes/No	No	Yes
Ionic strength	Yes/No	No	Yes
cleaning solvent	Yes/No	Methanol	Water

**Table 1.** Factors and values evaluated for the optimization of TP-SPE extraction. Bold values represent optimized values.

using methanol as the cleaning solvent. Figure 5 shows the scheme for the microextraction process with optimized parameters and variables.

When the extraction procedure for the standard solution and fortified urine sample solution was applied, an increase in the dexamethasone signal was observed compared with the standard solution without extraction. This behavior can be attributed to the phenomenon of absorption by the agglomerates. Therefore, the extraction efficiency was determined by comparing the signal of the fortified urine solution with that of the extracted standard solution. Under these conditions, an extraction percentage greater than 151% ( $n=2$ ) was estimated. Figure 6 shows representative chromatograms for the standard solution at 200 ng/mL (A), the urine sample fortified to the same concentration (B), and the urine blank (C). The absorption spectra of the chromatographic peaks confirm the selectivity of the proposed method.

Based on this result, it is possible to establish the presence of a matrix effect produced by the impurities in the sample that are retained in the agglomerate sorbent. Although a cleaning step was included in the extraction procedure, more was needed to avoid these effects. Finally, a visual comparison of the absorption spectra obtained in the chromatographic separation with the corresponding absorption spectrum obtained in the UV-Vis spectrophotometer during the extraction studies verifies the co-elution of interferences in the microextraction procedure. Standard addition calibration is best in this scenario when the proposed procedure is applied to determine dexamethasone levels in urine samples.

process enabled the production of amorphous agglomerates with a pore size of 2 nm and adequate physical characteristics. Thus, it is possible to establish that the process was highly effective, with minimum steps and low consumption of reagents. Several analytical techniques were applied to characterize the obtained agglomerates to establish their properties. The diffractogram obtained through X-ray diffraction showed that the agglomerates had a highly amorphous structure, which is characteristic of this type of compound because it does not have a marked crystalline structure. In the case of studies conducted through FTIR, characteristic bands were observed at 2929  $\text{cm}^{-1}$  corresponding to some vibrations C-H, and 1651  $\text{cm}^{-1}$  corresponding to vibrations C=C olephalic. Likewise, signals around 1510 and 1425  $\text{cm}^{-1}$  are assigned to the skeletal ones in aromatic rings. All of these bands are attributes of graphemic sheets in the CBA. The results of the BET analysis were auspicious for using carbon black agglomerates as sorbent material because a high surface area was observed due to the material's microporous nature. This was confirmed by the small pore size of 2.27 nm; therefore, it is concluded that the obtained material presents a micro/mesoporous structure. The SEM images of the material confirmed these findings.

Once the main characteristics of the obtained sorbent material were established, we focused on applying these agglomerates as sorbent materials for microextraction techniques based on the green analytical chemistry approach, with PT-SPE being selected. The extraction devices were made so that the least agglomerates were necessary to achieve the extraction. In this sense, tips with one and 5 mg were prepared, which allowed not only to reduce the amount of sorbent but also the cost of solvents necessary in the SPE procedure. During the preparation, an effort was made to ensure that the amount of sorbent had the least possible variation to obtain reproducible results during the analysis. The extraction percentages of the aqueous solutions of the studied compounds showed promising results for compounds such as paracetamol, caffeine, diazepam,

## Discussion

In this work, it was possible to obtain carbon black agglomerates based on vegetal material, thereby promoting waste recovery and using renewable raw materials, which are part of the principles of green chemistry. The synthesis

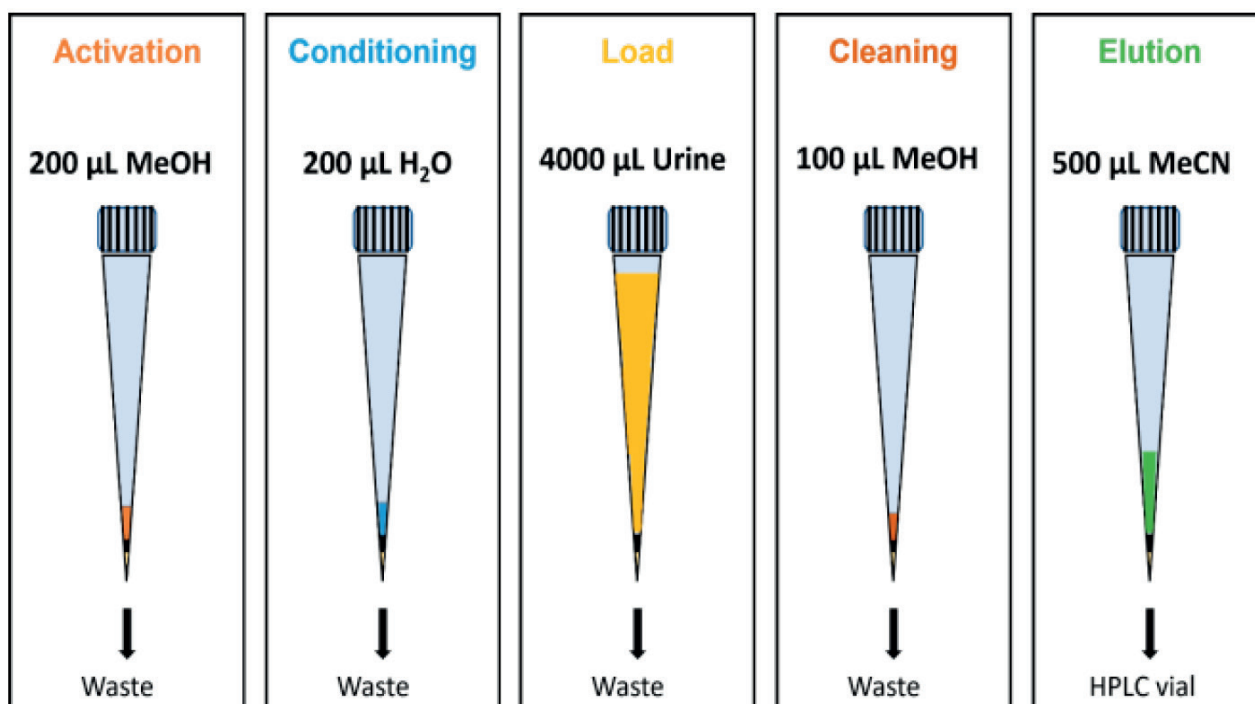


**Figure 5.** Schematic of the optimized microextraction procedure. For other experimental details, see the text.

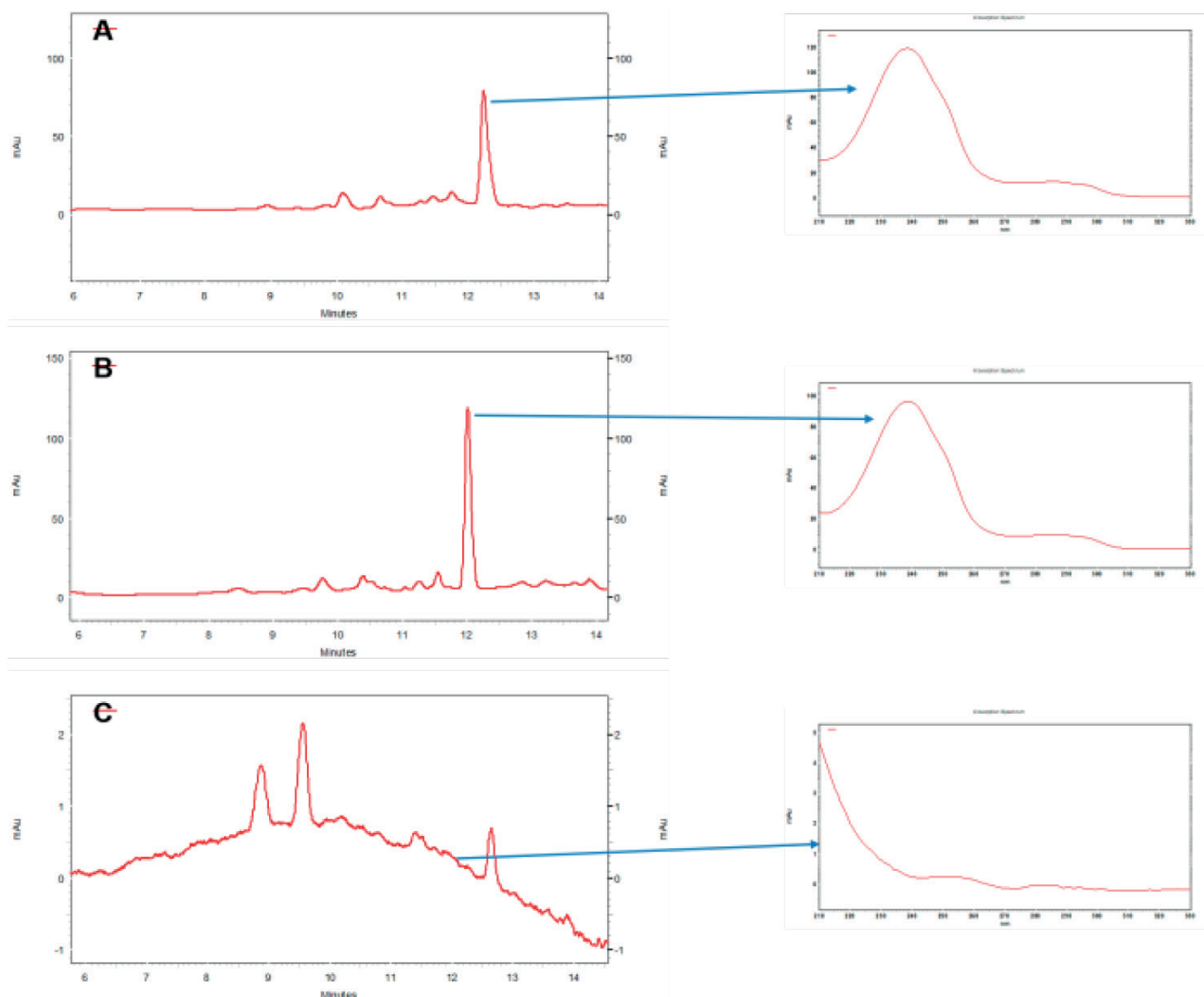


**Figure 6.** Representative chromatograms for the analysis of: (A) standard solution at 200 ng/mL; (B) urine sample fortified at 200 ng/mL; (C) urine blank. The absorption spectra of each chromatographic peak are shown.

and dexamethasone, with percentages more significant than 70% and, in the particular case of caffeine, up to 90%. Because of these results, our group is currently working on a study on the extraction of caffeine from energy drinks. Regarding molecules with low extraction percentages, variables such as modification of the ionic strength, solution pH, or sorbent amount could be studied to increase efficiency. Despite the promissory results, the drawback of the background signal caused by the matrix effect from the carbon black agglomerates could be a significant issue when actual samples, such as environmental or biological samples, are analyzed by the proposed procedure because these matrices have much interference.

In the last part of this study, PT-SPE was applied using CBA as a sorbent to extract dexamethasone in urine. For this, identification and quantification of the molecule were performed using HPLC-DAD. The chromatographic conditions made it possible to obtain the dexamethasone signal after 12 min, thus avoiding the co-elution of the interferences and impurities in the urine samples. Adequate linearity was obtained in the concentration range of five to 200 ng/mL of dexamethasone, for which it was necessary to inject up to 25  $\mu$ L of the standard solutions. The compound was identified through the retention time and comparison of the corresponding absorption spectra. Different parameters of the microextraction procedure were optimized to obtain a

high extraction efficiency. The application of PT-SPE demonstrated essential advantages from the viewpoint of green analytical chemistry, including low solvent consumption, automated process, high preconcentration factor, and reduced amount of agglomerate sorbent. This analytical methodology can help conduct pharmacokinetic or forensic studies where it is necessary to determine the concentrations of dexamethasone in urine. Although the high retention of the dexamethasone molecule in the CBA was satisfactory, the high matrix effect must be resolved when applying the proposed methodology. In the authors' opinion, a single-point standard addition calibration may be satisfactory for achieving the correct quantification of the analyte.

Applying carbon black agglomerates proved satisfactory for retaining pharmaceutical compounds in aqueous matrices. According to the authors, this is the first study to report the use of this type of sorbent material of vegetable origin. Developing new analytical methodologies based on the green analytical chemistry approach is possible because of its application as a sorbent material in different microextraction techniques. Our group is currently synthesizing and characterizing nanostructured materials using tamarind seeds, which have a much higher porosity and can yield promising results.



## Conclusions

The synthesis of carbon black agglomerates obtained from olive stone by-products of the olive oil industry was satisfactory by applying a fast, easy, and efficient procedure. Through this procedure, we obtained a material that presents specific suitable properties for its application as an extracting sorbent in various analytical matrices after being characterized by various analytical techniques. In the second stage of this study, PT-SPE was used as a novel microextraction technique for extracting pharmaceutical molecules with various chemical properties. The results were highly satisfactory for compounds such as paracetamol, caffeine, diazepam, and dexamethasone, with extraction percentages above 70%. Finally, the microextraction procedure was applied to analyze dexamethasone in urine by HPLC-DAD. The PT-SPE microextraction procedure proved straightforward, using only 5 mg of carbon black agglomerates and small amounts of solvents ( $\approx 1$  mL). Using a vacuum extraction chamber allows the process to be automated, performing up to twenty extractions in less than 5 min.

## Author Contributions

CConceptualization, FARR and HDPR; methodology, FARR and HDPR; software, EMOL; YNBG; FAOT; KABM; FARR and HDPR; validation, EMOL; YNBG; FAOT; KABM; FARR and HDPR; formal analysis, EMOL; YNBG; FAOT; KABM; FARR and HDPR; investigation, EMOL; YNBG; FAOT; KABM; FARR and HDPR; resources, EMOL; YNBG; FAOT; KABM; FARR and HDPR; data curation, EMOL; YNBG; FAOT; KABM; FARR and HDPR; writing—original draft preparation, EMOL; YNBG; FAOT; KABM; FARR and HDPR; writing—review and editing, EMOL; YNBG; FAOT; KABM; FARR and HDPR; visualization, EMOL; YNBG; FAOT; KABM; FARR and HDPR; supervision, FARR and HDPR; project administration, FARR and HDPR; funding acquisition, FARR and HDPR All authors have read and agreed to the published version of the manuscript.

## Funding

This research received no external funding.

## Acknowledgments

The authors appreciate the collaboration of Professor Alvaro Caballero Amores from the Department of Inorganic Chemistry and Chemical Engineering of the University of Cordoba for facilitating the carbon black agglomerates.

## Conflicts of Interest

The authors declare no conflicts of interest.

## Bibliographic references

1. European Commission, Official Journal of the European Union L, 20.10.2011, 2011, 275, 38.
2. Fasih Khalid, M.; Iqbal Khan, R.; Zaid Jawaid, M.; Shafiqat, W.; Hussain, S.; Ahmed, T.; Rizwan, M.; Ercisli, S.; Lelia Pop, O.; Alina Marc, R.; Nanoparticles: The Plant Saviour under Abiotic Stresses. *Nanomaterials*, 2022, 12, 395. <https://doi.org/10.3390/nano12213915>
3. Shah, M.M.; Ahmad, K.; Ahmad, B.; Shah, S.M.; Masood, H.; Ramzan Siddique, MA; Ahmad, R. Recent trends in green synthesis of silver, gold, and zinc oxide nanoparticles and their application in nanosciences and toxicity: a review. *Nanomaterials*, 2022, 12, 395. <https://doi.org/10.1007/s41204-022-00287-5>
4. Innocenzi, P.; Stagi, L.; Carbon dots as oxidant-antioxidant nanomaterials, understanding the structure-properties relationship. A critical review. *Nano Today* 2023, 50, 101837 <https://doi.org/10.1016/j.nantod.2023.101837>
5. Kumar Verma, S.; Kumar Das, A.; Gantait, Y.; Panwar, Y.; Kumar, V.; Brestic, M.; Green synthesis of carbon-based nanomaterials and their applications in various sectors: a topical review. *Carbon Letters*, 2022, 32:365–393 <https://doi.org/10.1007/s42823-021-00294-7>
6. Nayl, A. A.; Abd-Elhamid, A. I.; Alyc, A.A.; Bråse, S.; Recent progress in the applications of silica-based nanoparticles. *RSC Adv.*, 2022, 12, 13706. <https://doi.org/10.1039/D2RA01587K>
7. Yee, M.J.; Mubarak, N.M.; Abdullah, E.C.; Khalid, M.; Walvekar, R.; Karri, R.R.; Nizamuddin, S.; Numan, A.; Carbon nanomaterials based films for strain sensing application—A review, *Nanostructures and Nano-Objects.*, 2019, 18 <https://doi.org/10.1016/j.nanoso.2019.100312>.
8. Zheng, H.; Ding, J.; Zheng, S.; Yu, O.; Yuan, B.; Feng, Y.; Magnetic "one-step" quick, easy, cheap, effective, rugged and safe method for the fast determination of pesticide residues in freshly squeezed juice, *Journal of Chromatography A*, 2015, 1398, 1–10 <https://doi.org/10.1016/j.chroma.2015.04.021>
9. Andrade-Guel, M.; Reyes-Rodríguez, P.Y.; Cabello-Alvarado, C.J.; Cadenas-Pliego, G.; Ávila-Orta, C.A.; Influence of Modified Carbon Black on Nylon six Nonwoven Fabric and Performance as Adsorbent Material. *Nanomaterials* 2022, 12, 4247. <https://doi.org/10.3390/nano12234247>.
10. Messaoud, N.B.; Lahcen, A.A.; Dridi, C.; Amine, A.; Ultrasound assisted magnetic imprinted polymer combined sensor based on Carbon black and gold nanoparticles for selective and sensitive electrochemical detection of Bisphenol A. *Sensors & Actuators: B. Chemical* , 2018, 276, 304–312. <https://doi.org/10.1016/j.snb.2018.08.092>
11. Pereira Silva, L.; Almeida Silva, T.; Cruz Moraes, F.; Fatibello-Filho, O.; Carbon black-chitosan film-based electrochemical sensor for losartan. *Journal of Solid State Electrochemistry* , 2020, 24:1827–1834 <https://doi.org/10.1007/s10008-020-04541-1>
12. Sanjuan-Navarro, L.; Moliner-Martínez, Y.; P. Campíns-Falco. The state of art of nanocarbon black as analyte in a variety of matrices: A review. *Trends in Analytical Chemistry* , 2022, 157, 116769 <https://doi.org/10.1016/j.trac.2022.116769>
13. Hüffer, T.; Wagner, S.; Reemtsma, T.; Hofmann, T.; Sorption of organic substances to tyre wear materials: similarities and differences with other types of microplastic, *TrAC, Trends Anal. Chem.* , 2019, 113, 392–401. <https://doi.org/10.1016/j.trac.2018.11.029>.
14. Fulcheri, L.; Probst, N.; Flamant, G.; Fabry, F.; Grivei, E.; Bourrat, X.; Plasma processing: A step towards the production of new grades of Carbon black, *Carbon*, 2002, 40 [https://doi.org/10.1016/S0008-6223\(01\)00169-5](https://doi.org/10.1016/S0008-6223(01)00169-5)
15. Okoye, CO; Jones, I.; Zhu, M.; Zhang, Z.; Zhang, D.; Manufacturing of Carbon black from spent tyre pyrolysis oil – A literature review, *J. Clean. Prod.* , 2021, 279 <https://doi.org/10.1016/j.jclepro.2020.123336>
16. Almeida Silva, T.; Cruz Moraes, F.; Campos Janegitz, B.; Fatibello-Filho, O. Electrochemical Biosensors Based on Nanostructured Carbon Black: A Review. *J. Nanomater.*, 2017, 4571614, <https://doi.org/10.1155/2017/4571614>.
17. Plaza-Recobert, M.; Trautwein, G.; Pérez-Cadenas, M.; Alcañiz-Monge J.; Superactivated carbons by CO<sub>2</sub> activation of loquat stones. *Fuel Processing Technology*, 2017, 159, 345–352 <https://doi.org/10.1016/j.fuproc.2017.02.006>.
18. Filippín, A.J.; Luna, N.S.; Pozzi, T.; Pérez, J.D.; Obtención y caracterización de carbón activado a partir de residuos olivícolas y oleícolas por activación física. *Avances en Ciencias e Ingeniería.* , 2017, 8, 59–71.
19. Luna-Lama, F.; Morales, J.; Caballero, A.; Biomass Porous Carbons Derived from Banana Peel Waste as Sustainable Anodes for Lithium-Ion Batteries. *Materials*. 2021, 14, 5995. <https://doi.org/10.3390/ma14205995>.

20. Lian, F.; Yu, W.; Wang, Z.; Xing, B.; New Insights into Black Carbon Nanoparticle-Induced Dispersibility of Goethite Colloids and Configuration-Dependent Sorption for Phenanthrene. *Environ. Sci. Technol.*, 2019, 53, 661–670. <https://doi.org/10.1021/acs.est.8b05066>
21. Reddy, S.S.; Shukla, B.; Chakraborty, S.; Srihari, V.; Bhalerao, G. M.; Chandra Shekar, N. V.; Study on high-pressure behavior of spherical carbon black nanoparticles with core-shell structure. *Carbon Letters*, 2022, 32:1337–1344. <https://doi.org/10.1007/s42823-022-00355-5>
22. Duan, D.; Yuan, Z.; Jiang, Y.; Yuan, L.; Tai, H.; Amorphous carbon material of daily carbon ink: emerging applications in pressure, strain, and humidity sensors. *J. Mater. Chem. C*, 2023, 11, 5585–5600 <https://doi.org/10.1039/D3TC00016H>
23. Desai, F.J.; Uddin, M.N.; Rahman, M.M.; Asmatulu, R.; A critical review on improving hydrogen storage properties of metal hydride via nanostructuring and integrating carbonaceous materials. *International Journal of Hydrogen Energy*, 2023, 48, 50. <https://doi.org/10.1016/j.ijhydene.2023.04.029>
24. Boughbina-Portolés, A.; Sanjuan-Navarro, L.; Hakobyan, L.; Gómez-Ferrer, M.; Moliner-Martínez, Y.; Sepúlveda, P.; Campíns-Falcó, P.; Reliable assessment of carbon black nanomaterial of a variety of cell culture media for in vitro toxicity assays by asymmetrical flow field-flow fractionation. *Analytical and Bioanalytical Chemistry*, 2023, 415:2121–2132. <https://doi.org/10.1007/s00216-023-04597-8>
25. Guo, Y.; Ye, H.; Wang, H.; Wang, Q.; Fan, S.; Dou, H.; Asymmetrical flow field-flow fractionation combined with ultrafiltration: A novel and high-efficiency approach for separation, purification, and characterization of *Ganoderma lucidum* polysaccharides. *Talanta* 253, 2023, 124053. <https://doi.org/10.1016/j.talanta.2022.124053>
26. Ponce-Rodríguez, H. D.; Verdú-Andrés, J.; Herráez-Hernández, R.; Campíns-Falcó, P.; Innovations in Extractive Phases for In-Tube Solid-Phase Microextraction Coupled to Miniaturized Liquid Chromatography: A Critical Review. *Molecules*, 2020, 25, 2460; <https://doi.org/10.3390/molecules25102460>
27. López-Lorente, Á.I.; Valcárcel, M.; The third way in analytical nanoscience and nanotechnology: Involvement of nanotools and nanoanalytes in the same analytical process, *TrAC Trends Anal. Chem.* 75, 2016, 1–9. <https://doi.org/10.1016/j.trac.2015.06.011>
28. Badawy, M.E.I.; El-Nouby, M.A.M.; Kimani, P.K.; Lim, L.W.; Rabea, E.I.; A review of the modern principles and applications of solid-phase extraction techniques in chromatographic analysis. *Analytical Sciences*, 2022, 38:1457–1487. <https://doi.org/10.1007/s44211-022-00190-8>
29. Tsai, P.C.; Pundi, A.; Brindhadevi, K.; Ponnusamy, V.K.; Novel semi-automated graphene nanosheets based pipette tip assisted micro-solid-phase extraction as eco-friendly technique for the rapid detection of emerging environmental pollutant in waters. *Chemosphere*. 2021, Volume 276, 130031. <https://doi.org/10.1016/j.chemosphere.2021.130031>
30. Erzurumlu, Y.; Dogan, H.K.; Catakli, D.; Dexamethasone-stimulated glucocorticoid receptor signaling positively regulates the endoplasmic reticulum-associated degradation (ERAD) mechanism in hepatocellular carcinoma cells. *Steroids*, 2023, 195, 109238. <https://doi.org/10.1016/j.steroids.2023.109238>
31. Villar, J.; Ferrando, C.; Martínez, D.; Ambrós, A.; Muñoz, T.; Soler, J.A.; Aguilar, G.; Alba, F.; González-Higueras, E.; Conesa, L.A.; Martín-Rodríguez, C.; Díaz-Domínguez, F.J.; Serena-Grande, P.; Rivas, R.; Ferreres, J.; Belda, J.; Capilla, L.; Tallet, A.; Añón, J.M.; Fernández, R.L.; González-Martín, J.M.; Dexamethasone treatment for the acute respiratory distress syndrome: a multicentre, randomised controlled trial. *Lancet Respir Med*, 2020, 8, 267–76. [https://doi.org/10.1016/S2213-2600\(19\)30417-5](https://doi.org/10.1016/S2213-2600(19)30417-5)
32. Bagnati, R.; Ramazza, V.; Zucchi, M.; Simonella, A.; Leone F.; Analysis of Dexamethasone and Betamethasone in Bovine Urine by Purification with an "Online" Immunoaffinity Chromatography–High-Performance Liquid Chromatography System and Determination by Gas Chromatography–Mass Spectrometry. *Anal. Biochem.* 1996, 235, 119. <https://doi.org/10.1006/abio.1996.0103>
33. Mahdavi Ara, K.; Akhondpouramiri, Z.; Raofie, F.; Carrier mediated transport solvent bar microextraction for preconcentration and determination of dexamethasone sodium phosphate in biological fluids and bovine milk samples using response surface methodology. *Journal of Chromatography B*, 2013, 931, 148–156. <https://doi.org/10.1016/j.jchromb.2013.05.022>
34. Genangeli, M.; Caprioli, G.; Cortese, M.; Laus, F.; Petrelli, R.; Ricciutelli, M.; Sagratini, G.; Sartori, S.; Vittori, S.; Simultaneous quantitation of nine anabolic and natural steroidal hormones in equine urine by UHPLC-MS/MS triple quadrupole. *Journal of Chromatography B*, 2019, 1117, 36–40. <https://doi.org/10.1016/j.jchromb.2019.04.002>
35. Possi-Pezzali, T.; Chigome, S.; Rodríguez-Haralambides A.; Torto N.; Evaluation of electrospun fibers as solid-phase extraction sorbents for sample preparation in HPLC-MS/MS confirmatory doping control analysis of dexamethasone and betamethasone. *Anal. Methods*, 2013, 5, 4230–4237. <https://doi.org/10.1039/C3AY40606G>
36. Chen, D.M.; Tao, Y.F.; Liu, Z.Y.; Zhang, H.H.; Liu, Z.L.; Development of a liquid chromatography-tandem mass spectrometry with pressurized liquid extraction for determination of glucocorticoid residues in edible tissues, *J. Chromatography. B*, 2011, 879, 174–180. <https://doi.org/10.1016/j.jchromb.2010.11.039>
37. Huang, Y.; Zheng, Z.; Huang, L.; Yao, H.; Wu X. S.; Li, S.; Lin D.; Optimization of dispersive liquid-phase microextraction based on solidified floating organic drop combined with high-performance liquid chromatography for the analysis of glucocorticoid residues in food. *Journal of Pharmaceutical and Biomedical Analysis*, 2017, 138, 363–372. <https://doi.org/10.1016/j.jpba.2017.02.026>
38. Caballero, A.; Hernán, L.; Morales J.; Limitations of Disordered Carbons Obtained from Biomass as Anodes for Real Lithium-Ion Batteries. *ChemSusChem* 2011, 4, 658–663. <https://doi.org/10.1002/cssc.201000398>